Comparison of Curative Effects of Bone Marrow Mesenchymal Stem Cells and Melatonin on Bisphenol A Induced-Lung Fibrosis and Inflammation in Adult Male Albino Rats

Mai Hassan Ibrahim¹, Walaa A. Fadda², Rasha M. Salama²

¹Anatomy and Embryology Department, Faculty of Medicine, Benha University, Benha, Egypt ²Department of Anatomy and Embryology, Faculty of Medicine, Menoufia University, Egypt Corresponding author: Mai Hassan Ibrahim, Email: may.ibrahim@fmed.bu.edu.eg,

Phone no: +2 01145779734, **ORCID:** 0000-0001-5999-2612

ABSTRACT

Background: Bisphenol A (BPA), a common industrial compound, is recognized for its toxic effects on multiple organs, including the lungs, through oxidative stress and inflammatory pathways.

Aim: This study aimed to evaluate the deleterious impact of BPA on lung tissue in rats and to evaluate the potential curative roles of bone marrow mesenchymal stem cells (BM-MSCs) and melatonin in mitigating BPA-induced pulmonary damage. **Methods:** 50 adult male albino rats were randomly assigned into 5 groups (n=10 each): control, melatonin, BPA, BPA plus melatonin, and BPA plus BM-MSCs. Biochemical markers of oxidative stress (MDA, GSH, and SOD) were measured. Lung tissue samples were examined using histological (H & E and Masson's trichrome), immunohistochemical (TNF-α and COX-2), and ultrastructural (electron microscopy) analyses.

Results: The BPA group showed a significant increase in MDA and marked decreases in GSH and SOD compared to controls. Histologically, the lungs exhibited alveolar collapse, inflammatory infiltration, interstitial thickening, and collagen fiber accumulation. TNF-α and COX-2 expressions were markedly elevated, and electron microscopy revealed severe structural disruption. Co-treatment with melatonin or BM-MSCs ameliorated these alterations, with BM-MSCs producing a more pronounced restoration of biochemical, histological, and ultrastructural features.

Conclusion: BM-MSCs and melatonin effectively mitigated BPA-induced lung injury, with BM-MSCs demonstrating superior protective and reparative effects. The results indicate that BM-MSCs could serve as a promising therapeutic option for reducing lung fibrosis and inflammation caused by environmental toxins like BPA.

Keywords: BPA, TNF-α, COX-2, BM-MSCs, Melatonin.

INTRODUCTION

Bisphenol A (BPA) is a prominent synthetic industrial chemical that finds widespread and extensive application in the manufacturing sector. It is fundamentally utilized in the production of durable polycarbonate plastic resources and various forms of epoxy resin. Due to its molecular structure and biological activity, BPA is officially classified as an endocrine-disrupting chemical (EDC), meaning it possesses the ability to interfere with the body's hormonal systems [1].

BPA is an ingredient in water bottles, food packaging, infant bottles, medical equipment, personal care items, and metal can liners that can readily separate from plastics as a result of partial polymerization or hydrolysis of the polymers. High temperatures, acidic environments, or enzymatic processes can cause this separation [2].

Several studies correlated the inflammation, oxidative stress, and apoptosis as common pathways for BPA-induced lung injury [3]. The increased lung inflammatory responses, including the release of inflammatory cytokines, and increased oxidative stress, triggers DNA damage in type 2 epithelial cells [4]. The occurrence of DNA damage that precipitates cellular demise is an established, major mechanistic factor contributing to the advancement and increased severity of several critical pulmonary pathologies. These serious respiratory conditions, which include asthma, chronic

obstructive pulmonary disease (COPD), lung cancer, and various fibrotic lung diseases, all share this underlying mechanism where the disruption of genomic integrity drives their progressive, detrimental course [5]. The primary mechanism by which Bisphenol A (BPA) induces lung tissue damage is through direct DNA damage to epithelial cells. This damage occurs due to the excessive generation of reactive oxygen and nitrogen species (ROS and RNS), which ultimately results in cell death [6]. Furthermore, ROS can modify proteins and organelles, and generate hydroxyl radicals that are capable of damaging DNA. This cascade subsequently triggers inflammation, adverse immunological responses, cellular demise, and the development of immune-related lung disorders [7]. Tissue fibrosis is responsible for worldwide morbidity and mortality. Additionally, lung fibrosis has miserable prognosis and treatment options. However, recent advancements in alternative therapies have displayed encouraging outcomes in the management of lung fibrosis [8].

Melatonin is a hormone that was synthesized in the human body by the pineal gland, found throughout the body, and responsible for a variety of purposes, including regulations of mood, sleep, and immune system, and has powerful antioxidant and anti-inflammatory effects ^[9]. Also, has the capability to scavenge free radicals, induces multiple antioxidant enzymes and inhibits pro-oxidant enzymes, so it protects cellular components against oxidative damage ^[10].

Received: 27/05/2025 Accepted: 29/07/2025 Numerous scientific researches have shown a great deal of interest in bone marrow mesenchymal stem cells (BM-MSCs) because they are easy to extract, have remarkable proliferation capability, can differentiate into several cell types, and secrete signaling chemicals. These qualities make them an excellent choice for autologous stem cell-based replacement therapy [11]. BM-MSCs prove great promise for the field of regenerative medicine as it can enhance tissue regeneration in many organs, including the bone, cartilage, liver, heart, skin, and neural tissue and treatment of lung fibrosis because of their distinctive regenerative, anti-apoptotic and anti-inflammatory effects [12].

Thence, the current study aimed to investigate the toxicological effects of the industrial chemical Bisphenol A (BPA) on the pulmonary health of adult male albino rats. Concurrently, it was meant to propose and assess the therapeutic efficacy of BM-MSCs and melatonin in alleviating the observed BPA-induced lung pathology.

MATERIAL AND METHODS

Experimental chemicals: Bisphenol A (BPA): was obtained from Sigma, Egypt (Sigma, St. Louis, MO, USA). Powder was gavaged in a dose of 50 mg/kg after being freshly dispersed in corn oil (10 mg BPA: 1ml corn oil) for 14 days for each rat based on its weight [13].

Melatonin: was obtained from Egypt (Manufactured by PURITAN'S PRIDE, INC. Ronkonkoma, NY 11779 U.S.A.) in the form of tablets, each tablet contained 5 mg melatonin. The tablet was crushed and dissolved in100 ml saline, so each 1ml saline contained 0.05 mg melatonin. Using an endogastric tube, melatonin was administered orally at a dose of 5 mg/kg once per day for 14 days for each rat based on its weight [14].

Experimental animals: Fifty adult male albino rats (180-200 g/each) were applied in this experiment. Rats were shielded in separate well aerated clean containers, at room temperature and under strict care and hygienic conditions with free use to food and water. The experiment was acted upon in Faculty of Medicine, Benha University.

Experimental protocol: Rats were separated into five experimental groups, which were as follows:

- **I. Control group (n=10):** It was more classified into five subgroups (2 rats each):
 - **Subgroup Ia:** Rats were left without any treatments throughout the experiment, and used as donor for BM-MSCs.
 - **Subgroup Ib:** Each rat was gavaged 20 ml/day saline (as melatonin vehicle) for 14 days.
 - **Subgroup Ic:** Each rat was swallowed 1 ml/day corn oil (as BPA vehicle) for 14 days.

- **Subgroup Id:** Each rat was wallowed 20 ml/day saline and 1 ml/day corn oil for 14 days.
- **Subgroup Ie:** Each rat had an intraperitoneal injection of 0.5 ml PBS on 1st day of the experiment (vehicle for BM-MSCs).
- **II. Melatonin group** (**n=10**): Each rat swallowed 5 mg/kg/day melatonin dissolved in saline as previously stated for 14 days.
- III. BPA group (n=10): Each rat was swallowed 50 mg/kg/day BPA dispersed in corn oil as previously stated for 14 days.
- **IV. BPA plus melatonin group (n=10):** Each rat was swallowed 50 mg/kg/day BPA dispersed in corn oil as previously stated for 14 days, then on the 14th day was swallowed 5 mg/kg/day melatonin dissolved in saline as previously stated for 14 days.
- **V. BPA plus BM-MSCs group (n=10):** Each rat received a single intraperitoneal shot of 2×10^6 cells/rat BM-MSCs dissolved in PBS on the 14th day, after it swallowed 50 mg/kg/day BPA dispersed in corn oil as previously stated, for 14 days.

All rats were sacrificed after 14 days or on the 28th day from beginning of the experiment according to each group.

Experimental protocol

Bone marrow mesenchymal stem cells (BM-MSCs): BM-MSCs were acquired from the Central Research Unit of Benha University Hospital, Egypt. The cells were harvested from the bone marrow of the femurs and tibiae of male rats that were 6 weeks old. Prior to use, the BM-MSCs were fluorescently labeled with the PKH67 Red Fluorescent Cell Linker.

The isolated MSCs were cultured in Dulbecco's Modified Eagle Medium (DMEM), which was procured from Sigma. All subsequent experiments were conducted using confluent cultures, a state that was typically achieved between the 12th and 14th day of the culture period. For the entirety of the experimental procedures, cells at passage 3 were consistently employed. The in vitro identification of the MSCs was confirmed during routine culture research by observing the cells using an inverted microscope (Olympus CKX53), where they were confirmed to appear as characteristic spindle-shaped cells. For the in vitro detection and tracking of the transplanted cells, lung tissue samples were analyzed using a fluorescent microscope (Olympus BX50F4, No. 7M03285, Tokyo, Japan) to identify the presence of the PKH67-stained cells (Fig. 1). The extracted cells utilized in the third passage were specifically labeled with the Red fluorescent protein (PKH67-Sigma) [12].

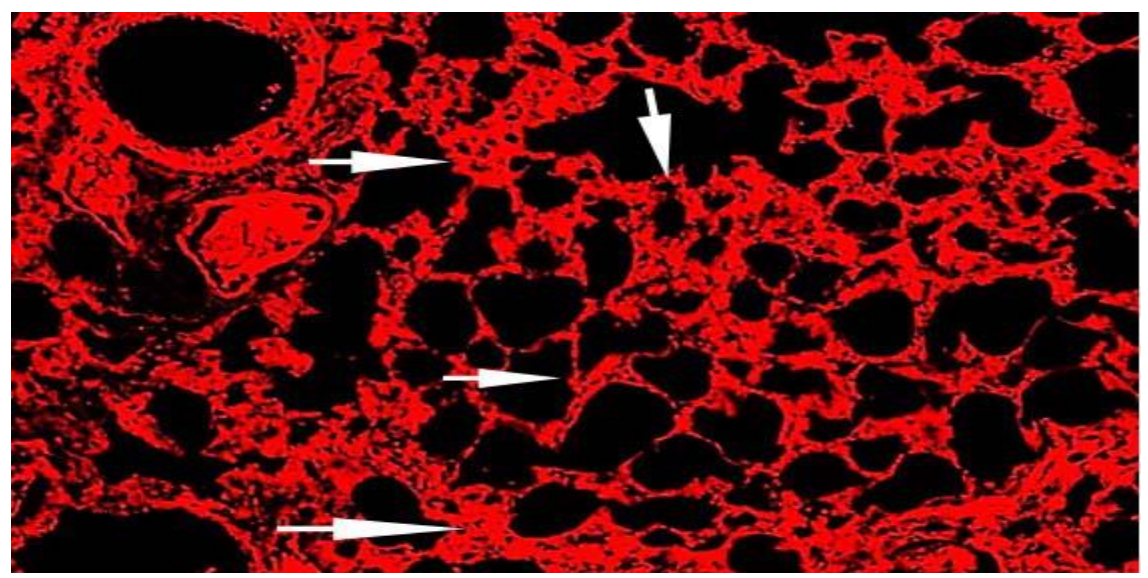


Figure (1): A photomicrograph of a section of the adult rat lung of BPA plus BM-MSCs group exhibiting positive red autofluorescence PKH26 fluorescent dye labeled MSCs (arrows).

Serum biochemical studies

Blood samples collection: Just before sacrifice samples of venous blood from retro-orbital plexus (3 ml/rat in each study group), under light anesthesia by thiopental at a dose of 50 mg/kg body weight, were obtained from animals using capillary glass tubes. Blood samples were left to clot at room temperature for 30 minutes. Then, the serum was separated via centrifugation for at least 15 minutes at 3000g and 4 °C. The detached serum was reserved at -80 °C till used [15].

Serum biochemical estimation of lipid peroxidation and oxidative stress markers: Serum content of malondialdehyde (MDA) (lipid peroxidation end product), reduced glutathione (GSH), and superoxide dismutase (SOD) levels were estimated. Commercially available colorimetric activity assay kits (Bio-diagnostics, Giza, Egypt) were utilized.

MICROSCOPIC STUDIES

After the animals were sacrificed. The following procedures were performed on each rat in each research group: The thoracic cavity was opened, the lungs were quickly excised, and washed in an ice-cold saline solution for the following studies:

Light microscopic studies: Right lungs were fixed by being immersed in 10% formalin solution 24 hours period prior to making paraffin blocks, that were prepared through washing in 0.1 M phosphate buffer saline (SBS), dehydrating in ascending grades of alcohol, clearing, and then paraffin embedding ^[16]. Afterwards, serially cut slices of 4-5 μm thick tissue were handled for histological and immune-histochemical analysis under a light microscope (Olympus, Japan) under x100 and x200 magnifications.

- **I. Histological staining:** Paraffin-embedded lung slices stained by Hematoxylin and eosin (H & E) and Masson's trichrome stain to demonstrate collagen fibers [16]
- **II. Immunohistochemical staining:** Using duplicate 4-5 μm thick lung tissue slices, the paraffin-embedded tissue blocks of formalin fixed lung tissues were immunestained using the streptavidin biotin-peroxidase technique ^[16] for recognition of:
- 1. Tumor necrosis factor alpha (TNF- α) immunoexpression: As an inflammatory marker, primary monoclonal antibody utilized was the mouse anti-TNF- α (1:300 with PBS). Mayer's hematoxylin was used to counter-stain sections. Cells appeared with brown cytoplasm, and tonsil was used as a positive control for anti-TNF [16].
- **2.** Cyclooxygenase-2 (COX-2) immunoexpression: As an inflammatory marker, using rabbit and goat polyclonal primary antibody and an anti-rabbit and anti-goat secondary antibody for COX-2 (1:500 dilution, Abcam, UK). Counterstain was performed by Mayer's hematoxylin and mounted on crystal. Negative controls were involved by incubating sections with antibody dilution buffer rather than the primary antibody [16].

Electron microscopic study: Left lungs from all rat groups where processed, and embedded by routine protocol. Semithin sections (1 μm thick) were obtained and stained by 1% toluidine blue followed by light microscopy inspection. On copper grids, ultrathin retinal sections (80-90 nm) were mounted, before being stained with uranyl acetate as well as lead citrate ^[17]. Examination of the grids of the lung specimens was done by using Jeol electron microscope (Seo-Russia) in electron microscopic unit, Faculty of Medicine, Benha University.

Morphometrical studies:

- 1. Mean area percentage of collagen fibers were counted via light microscopic examination of the Masson's trichrome stain photographs ×200.
- 2. Mean area percent of TNF- α and COX-2 positive immunoreactive cells were counted using light microscopic analysis of the immune-stained images $\times 200$.

Ethical approval: The experimental procedures were conducted within the facilities of the Faculty of Medicine, Benha University. Formal authorization for the execution of this study was secured from the Research Ethics Committee of the affiliated institutes, ensuring all aspects of the research adhered to established ethical standards and guidelines (RC 4-3-2025).

Statistical analysis

All data analysis was executed utilizing the SPSS software version 20 (SPSS Inc., Illinois, USA, Chicago). The quantitative results of the study were descriptively summarized and presented as the mean followed by standard deviation (SD). For the inferential statistical assessment of differences across multiple independent groups, the one-way analysis of variance (ANOVA) was initially implemented. When the ANOVA yielded a statistically significant result, the Post hoc Tukey's test was subsequently employed to perform pairwise comparisons among the group means while controlling

for the family-wise error rate. The statistical outcome was prospectively deemed significant when the calculated P value was less than or equal to 0.05.

RESULTS

All examined parameters between subgroups of control group and melatonin group revealed non-significant difference. Thus, all subgroups of control group and melatonin group were referred to as the control group. Biochemical results: Regarding the mean tissue levels of MDA, there was a highly significant increase in BPA group as compared to the control group (P = 0.000). However, the BPA plus melatonin and BPA plus BM-MSCs groups demonstrated high significant decrease compared to the BPA group (P = 0.001 and P = 0.000, respectively). However, the BPA plus BM-MSCs group revealed an insignificant increase when compared to the control group (P = 1.00). Regarding the mean tissue level of GSH & SOD, there was a highly significant decrease in the BPA group as compared to the control group (P =0.000 for both SOD & GSH). Also, the BPA plus Melatonin and BPA plus BM-MSCs groups demonstrated a high significant increase compared to the BPA group (P = 0.008 and P = 0.000, respectively for SOD & P = 0.000 and P = 0.000 for GSH). However, the BPA plus BM-MSCs group revealed an insignificant decrease when compared to the control group (P = 1 for SOD & P = 0.57for GSH) (Table 1).

Table (1): Effect of Bisphenol A, BPA+Melatonin, and BPA+Bone Marrow Mesenchymal Stem Cells on oxidative stress markers (MDA, SQD, and GSH) in lung tissue of rats

	Group I (Control group)	Group III (BPA group)	Group IV (BPA plus Melatonin group)	Group V (BPA plus BM-MSCs group)	P value
MDA(nmol/ml) Mean ±SD Nmol/gm tissue	123 ± 0.35	3.9 ±0.3	$2.17 {\pm}~0.2$	$1.4{\pm}0.3$	$\begin{array}{c} 0.000^{a} \\ 0.001^{b} \\ 0.000^{c} \\ 0.03^{d} \\ 1.00^{e} \\ 0.09^{f} \end{array}$
SOD((U/mg) Mean ±SD U/gm	3.5 ± 0.35	1.57 ± 0.25	2.6 ± 0.15	3.2± 0.3	0.000 ^a 0.008 ^b 0.001 ^c 0.03 ^d 1.00 ^e 0.2 ^f
GSH(mmol/L) Mean ±SD Nmol/mg tissue	2.47 ± 0.15	0.9 ±0.1	2 ± 0. 1	2.27 ± 0.15	0.000 ^a 0.000 ^b 0.000 ^c 0.02 ^d 0.57 ^e

Number of samples (10 in each group), MDA: malondialdehyde, SOD: superoxide dismutase & GSH: Glutathione. Values are presented as mean \pm SD, a Comparison between the control group and the BPA group, b Comparison between the BPA group and BPA + Melatonin group, c Comparison between BPA group and BPA plus BM-MSCs group,d Comparison between control group and BPA + Melatonin group, e Comparison between the control group and BPA plus BM-MSCs group, f Comparison between BPA + Melatonin group and BPA plus BM-MSCs group.

MICROSCOPIC RESULTS

Histological light microscopic, morphometrical and statistical results: H&E stain: Sections of the control group stained with H & E exhibited variable sized alveoli and alveolar sacs separated by delicate interalveolar septa housing blood capillaries. Bronchioles were lined with columnar cells arranged in folded mucosa, surrounded by thin smooth muscle fibers coat. The alveolar walls were lined by pneumocytes type I, squamous epithelial cells with flattened nuclei and pneumocytes type II that appeared cuboidal (rounded) cells with rounded nuclei, located at the angular junction of the alveolar walls (Figures 2A and 3A). However, H&E-stained sections of the BPA group displayed lung interstitium consolidation, and significant inflammatory cellular infiltration. The majority of the alveoli were collapsed. It was observed that the bronchiolar mucosa was discontinuous. Sloughed bronchiolar mucosal cells with dark, tiny nuclei and eosinophilic exudate were found. Lung interstitium

contained acidophilic homogeneous material. Additionally, extravasated RBCs and inflammatory cells such as neutrophils and eosinophils were observed in the alveolar spaces. Interalveolar septum appeared thickened containing congested dilated capillaries with inflammatory cells and thickened wall (Figures 2B,2C, 3B and 3C). By using melatonin with BPA in BPA plus Melatonin group, lung tissue reclaimed almost all its histological features. Intact continuous normal bronchiolar layers were noticed. Patent alveoli bordered by pneumocytes type I and pneumocytes type II appeared. However, there was slight thickening in the interalveolar septa with few congested blood capillaries and few inflammatory cellular infiltrate that were still present (Figures 2D and 3D). Moreover, H & E-stained sections of the BPA plus BM-MSCs group demonstrated features similar to those of the control group, however few inflammatory cellular infiltrate were still present (Figures 2E and 3E).

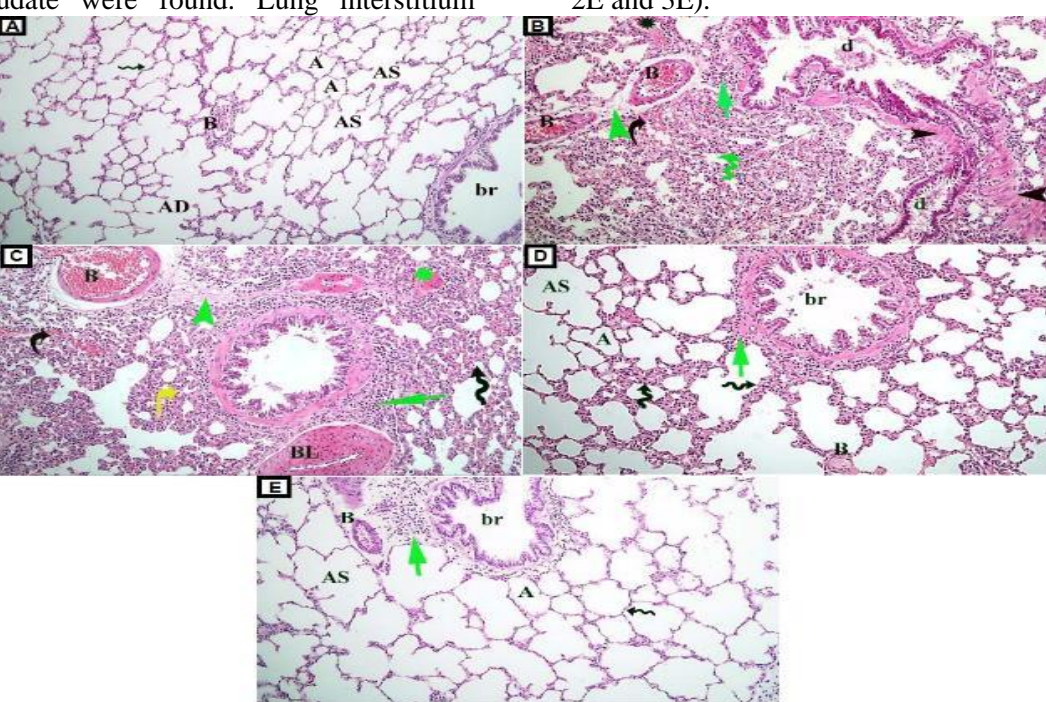


Fig. (2): A photomicrograph of H & E stain (×100) of the adult rat lung.

(A) Group I (control group) showed alveoli (A) and alveolar sacs (AS) separated by delicate interalveolar septa (zigzag arrow) housing blood capillaries (B). Alveolar duct (AD). Bronchioles (br) were lined with columnar cells arranged in folded mucosa, surrounded by thin smooth muscle fibers coat. (B) Group III (BPA group) revealed lung interstitium consolidation, with thickened intealveolar septa (zigzag arrow) and significant inflammatory cellular infiltration (green arrow). The majority of the alveoli were collapsed. Bronchiolar mucosa was discontinuous. Sloughed bronchiolar mucosal cells (d) and eosinophilic exudate were found (asterstick). Congested blood vessels (B), extravasated red blood cells (curved arrow), and fibrosis (black arrow head) were also observed. (C) Group III (BPA group) illustrated congested dilated blood vessels (B), thickened wall blood vessel (BL) leukocytic inflammatory infiltrate (green arrow), extravasated red blood cells (curved arrow) and perivascular fibrosis (arrow head) were also observed. The majority of the alveoli were collapsed (right angle arrow) with thickened intealveolar septa (zigzag arrow) and eosinophilic exudate were found (asterstick). (D) Group IV (BPA plus Melatonin group) demonstrated alveoli (A) and alveolar sacs (AS) separated by slightly thick interalveolar septa (zigzag arrow) housing blood capillaries (B). Bronchioles (br) were lined with columnar cells arranged in folded mucosa, surrounded by thin smooth muscle fibers coat but there is still some inflammatory cellular infolded mucosa, surrounded by thin smooth muscle fibers coat but there was still some inflammatory cellular infolded mucosa, surrounded by thin smooth muscle fibers coat but there was still some inflammatory cellular infolded mucosa, surrounded by thin smooth muscle fibers coat but there was still some inflammatory cellular infiltrate (green arrow).

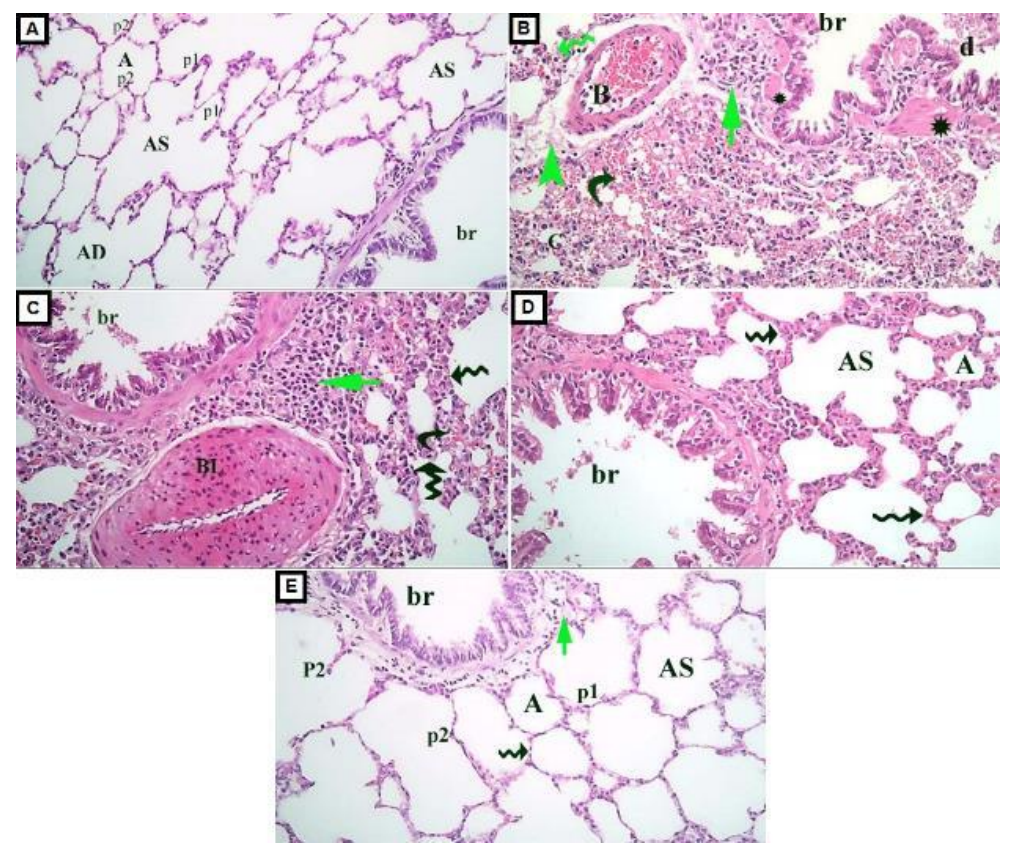


Fig. (3): A photomicrograph of H&E stain (×200) of the adult rat lung;

- (A) Group I (control group) showed alveoli (A), Alveolar duct (AD) and alveolar sacs (AS) separated by delicate interalveolar septa (zigzag arrow) housing blood capillaries (B). Bronchioles (br) were lined with columnar cells arranged in folded mucosa, surrounded by thin smooth muscle fibers coat. Alveolar walls lined by pneumocytes I(p1); squamous cells with flattened nuclei and pneumocytes II (P2) cells with rounded nuclei, located at the angular junction of the alveolar walls.
- (B) Group III (BPA group) revealed lung interstitium consolidation, with thickened intealveolar septa (zigzag arrow) and significant inflammatory cellular infiltration (green arrow). The majority of the alveoli were collapsed (c). Bronchiolar mucosa was discontinuous (br). Sloughed bronchiolar mucosal cells (d) and eosinophilic exudate were found (asterstick). Congested blood vessels (B), extravasated red blood cells (curved arrow), and fibrosis (black arrow head) were also observed.
- (C) Group III (BPA group) illustrated thickened wall blood vessel (BL) leukocytic inflammatory infiltrate

- (green arrow and extravasated red blood cells (curved arrow) were also observed. Thickened intealveolar septa (zigzag arrow) and eosinophilic exudate were found (asterstick).
- (**D**) Group IV (BPA plus Melatonin group)) demonstrated alveoli (A) and alveolar sacs (AS) separated by slightly thick interalveolar septa (zigzag arrow). Bronchioles (br) were lined with columnar cells arranged in folded mucosa, surrounded by thin smooth muscle fibers coat but there was still some inflammatory cellular infiltrate.
- (E) Group V (BPA plus BM-MSCs group) showed alveoli (A) and alveolar sacs (AS) separated by delicate interalveolar septa (zigzag arrow). Alveolar walls lined by pneumocytes I(p1), squamous cells with flattened nuclei and pneumocytes II (P2) cells with rounded nuclei, located at the angular junction of the alveolar walls Bronchioles (br) were lined with columnar cells arranged in folded mucosa, surrounded by thin smooth muscle fibers coat but there was still some inflammatory cellular infiltrate (green arrow).

Masson's trichrome stain: Histological examination, utilizing Masson's trichrome staining, was performed to assess the extent of pulmonary collagen deposition across the different treatment groups, providing a quantitative measure of fibrosis. The stained sections derived from the control group revealed a baseline state characterized by a very minimal amount of collagen fibers, which were strictly confined to the delicate interalveolar septa (Figure 4A). This minimal presence represents the normal, healthy architecture of the lung parenchyma. In sharp contrast, tissue sections obtained from the BPA group representing the chemically injured lung—clearly demonstrated a pronounced increased amount of collagen fibers. This pathological accumulation was evident within the interalveolar septa and notably concentrated in the connective tissue surrounding the bronchi and encircling the walls of the pulmonary blood vessels (Figure 4B).

This severe and widespread deposition strongly indicated the development of significant BPA-induced pulmonary fibrosis. Therapeutic interventions, however, produced varying degrees of mitigation. Specifically, the BPA plus Melatonin group exhibited a moderate reduction in pathology, illustrating a moderate amount of collagen fibers interspersed between the alveoli and still present around the blood vessels (Figure 4C), suggesting a partial protective effect. Most notably, the BPA plus BM-MSCs group sections demonstrated an almost complete reversal of the fibrotic state, revealing only a very minimal amount of collagen fibers specifically within the interalveolar septa (Figure 4D). This finding suggests that the infusion of Bone Marrow-Mesenchymal Stem Cells was highly effective in preventing or resolving the chemicallyinduced collagen overexpression and lung remodeling.

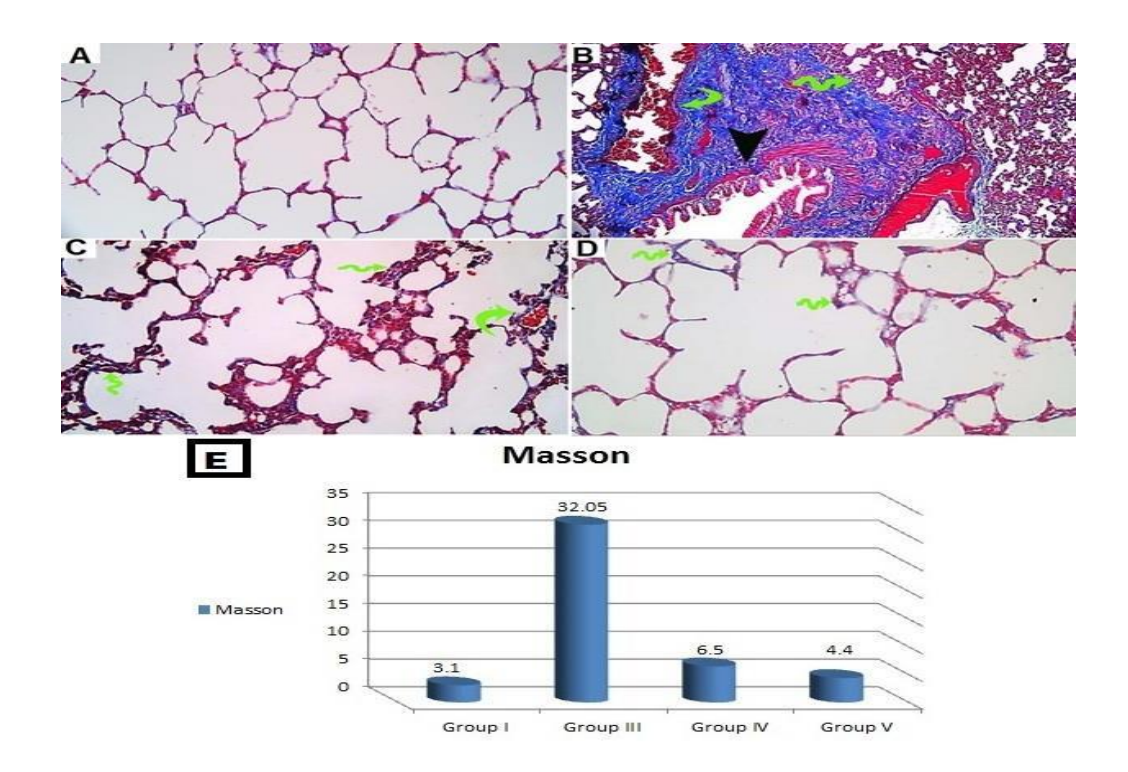


Fig. (4): A photomicrograph of Masson's Trichrome stain (×200) of the adult rat lung;

(A) Group I (Control group) showed very minimal amount of collagen fibers in the interalveolar septa. (B) Group III (BPA group) revealed increased amount of collagen fibers around bronchi (arrow head), around blood vessels (curved arrow) and in the alveolar septa (zigzag arrow). (C) Group IV (BPA plus Melatonin group) demonstrated a moderate amount of collagen fibers in between the alveoli (zigzag arrow) and surrounding blood vessels (curved arrow). (D) Group V (BPA plus BM-MSCs group) showed a minimal amount of collagen fibers in between the alveoli (Zigzag arrow). (E) Histogram showed area % of collagen fiber deposition in different groups.

Concerning the morphological results of the mean area % of collagen fiber deposition, there was a highly significant increase in the BPA group compared to the control group (P=0.000). While, the BPA plus melatonin group demonstrated a high significant decline in comparison with the BPA group (P=0.000) and the BPA plus BM-MSCs group showed a highly significant decrease when compared to the BPA group (P=0.000), while displayed a non-significant increase when compared to the control group (P=0.95) (Table 2, Figure 4E).

Table (2): Effect of Bisphenol A, BPA+Melatonin, and BPA+ bone marrow mesenchymal stem cells on collagen fiber

deposition in lung tissue (Masson's trichrome stain morphometric analysis)

	Group I (Control group)	Group III (BPA group)	Group IV (BPA plus Melatonin group)	Group V (BPA plus BM-MSCs group)	P value
Area % of collagen fiber deposition mean ± SD	3.1 ± 1	32.05 ± 1.1	6.5 ± 0.7	4.4 ± 1.2	0.000 a 0.000 b 0.000 c 0.04d 0.95e 0.3f

a Comparison between the control group and the BPA group, b Comparison between the BPA group and BPA + Melatonin group, c Comparison between BPA group and BPA plus BM-MSCs group, d Comparison between control group and BPA + melatonin group, e Comparison between the control group and BPA plus BM-MSCs group, f Comparison between BPA + melatonin group and BPA plus BM-MSCs group.

Immunohistochemistry: TNF- α ; stained sections of the lung tissue of the control group showed negative expression (Figure 5A). However, BPA group; stained lung sections demonstrated increased brown coloration in the inter-alveolar septa that indicated strong positive cytoplasmic expression (Figures 5B). Whereas sections of BPA plus melatonin group showed less obvious expression (Figure 5C), and that of BPA plus BM-MSCs group showed negative TNF α expression (Figure 5D).

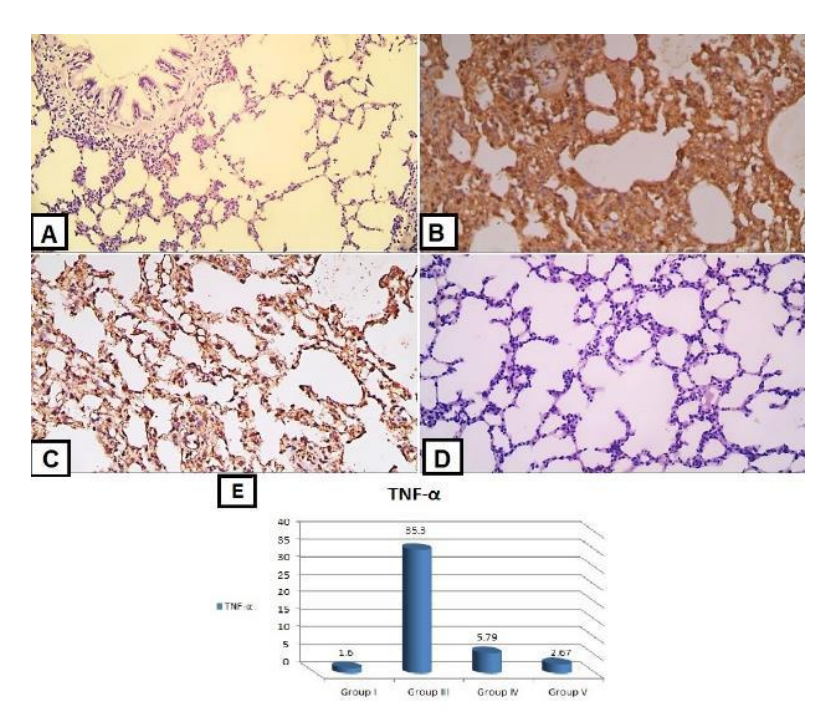


Fig. (5): TNF- α immunostained (×200) photomicrograph of the rat lung.

(A) Group I (control group) demonstrated very minimal TNF α expression. (B) Group III (BPA group) revealed increased brown coloration of cytoplasm, which indicates a strong positive cytoplasmic TNF α reaction. (C) Group IV (BPA plus melatonin group) showed moderate TNF α expression. (D) Group V (BPA plus BM-MSCs group) illustrated minimal TNF α expression. (E) Histogram showed area % of TNF α immunoreactivity.

Concerning the % positive area of TNF α immunoreactivity, the BPA group illustrated a highly significant rise compared to the control group (P= 0.000). While, the BPA plus melatonin group showed a high significant decrease in comparison to the BPA group (P= 0.000). Moreover, the BPA plus BM-MSCs group demonstrated a highly significant decrease when compared to the BPA group (P= 0.000) and displayed a non-significant rise when compared to the control group (P= 1) (Table 3 and figure 5E).

COX-2; stained sections of the lung tissue of the control group showed negative expression (Figure 6A). However, BPA group-stained lung sections demonstrated increased brown coloration in the inter-alveolar septa that indicated strong positive cytoplasmic expression (Figures 6B). Whereas sections of BPA plus melatonin group showed less obvious expression (Figure 6C), and that of BPA plus BM-MSCs group showed minimal COX-2 expression (Figure 6D).

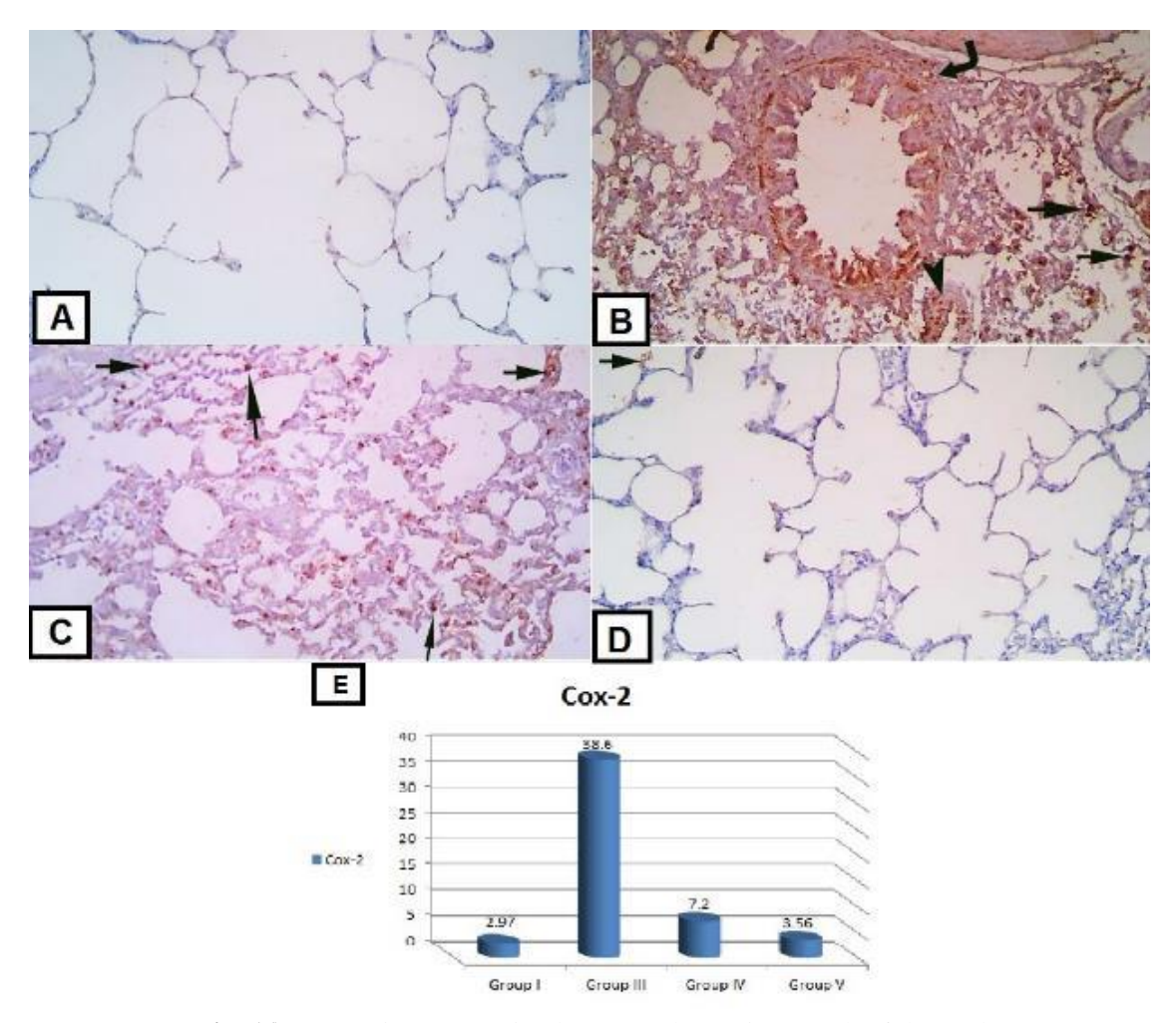


Fig. (6): Cox-2 immunostained (×200) photomicrograph of the rat lung.

(A) Group I (the control group) demonstrated very minimal Cox-2 expression. (B) Group III (BPA group) revealed increased brown coloration inbetween alveoli (black arrows), around bronchioles (right angle arrow) & around blood vessels (arrow head) which indicated a strong positive cytoplasmic Cox-2 expression. (C) Group IV (BPA plus melatonin group) showed moderate Cox-2. expression (black arrows), (D) Group V (BPA plus BM-MSCs group) illustrated minimal Cox-2 expression. (black arrow), (E) Histogram showed area % of Cox-2 immunoreactivity.

Regarding the mean area % of COX--2 immunoreactivity in the BPA group, it illustrated a highly significant increase compared to the control group (P=0.000). While, the BPA plus melatonin group showed significant decrease in comparison with the BPA group (P=0.000). Also, the BPA plus BM-MSCs group demonstrated a highly significant decrease when compared to the BPA group (P=0.000) and displayed a non-significant rise when compared to the control group (P=1) (Table 3 and figure 6E).

Table (3): Effect of Bisphenol A, BPA+Melatonin, and BPA+bone marrow mesenchymal stem cells on TNF-α and COX-

2 immunoreactivity in lung tissue

	Group I (Control group)	Group III (BPA group)	Group IV (BPA plus Melatonin group)	Group V (BPA plus BM-MSCs group)	P value
TNFα mean ±SD	1.6 ± 0.3	35.3± 1.04	5.79± 1.03	2.67 ± 0.4	0.000^{a} 0.000^{b} 0.000^{c} 0.03^{d} 1.00^{e} 0.06^{f}
Cox-2 mean ±SD	2.97 ± 0.78	38.6 ± 2.3	7.2 ±0.9	3.56 ± 0.6	0.000^{a} 0.000^{b} 0.000^{c} 0.04^{d} 1.00^{e} 0.06^{f}

a Comparison between the control group and the BPA group, b Comparison between the BPA group and BPA + Melatonin group, c Comparison between BPA group and BPA plus BM-MSCs group, d Comparison between control group and BPA + Melatonin group, e Comparison between the control group and BPA plus BM-MSCs group, f Comparison between BPA + Melatonin group and BPA plus BM-MSCs group.

Histological electron microscopy results:

Ultrathin sections of the lung tissue from the control group displayed a normal alveolar architecture. The alveoli were consistently lined by both type I and type II pneumocytes. Within the inter-alveolar septa, a normal blood capillary was observed. The type I pneumocyte was characterized by an elongated, euchromatic nucleus encased by a very thin rim of cytoplasm. In contrast, the type II pneumocyte exhibited a rounded, euchromatic nucleus and an apical surface covered with microvilli. Its cytoplasm was notable for containing lamellar bodies with distinct concentric lamellae, as well as mitochondria featuring prominent cristae (Figure 7 A and B).

An electron microscopic examination of the BPA group revealed marked alterations in the alveolar architecture. The type I pneumocytes exhibited irregular, heterochromatic nuclei and vacuolated cytoplasm, indicating cellular distress. Within the inter-alveolar septa, congested blood vessels were clearly observed. The alveolar spaces contained eosinophil cells with their characteristic granules, along with multiple alveolar macrophages that displayed a kidney-shaped nucleus and numerous lysosomes. Type II pneumocytes containing irregular heterochromatic shrunken nuclei, empty lamellar bodies. mitochondria. blunted swollen

microvillous border and the interalveolar septa appeared thickened having more collagen fibers (Figure 7 C, D, E & F). While, an electron microscopic examination of the BPA Plus Melatonin group showed pneumocytes type I having oval euchromatic nuclei and thin rim of cytoplasm. Alveolar macrophage with lamellipodia and kidney shaped nucleus was observed within alveolus. Pneumocytes type II possessed rounded nuclei, lamellar bodies with some vacuolation, and rounded mitochondria. Wide alveolar space bounded with thin interalveolar septum having few collagen fibers (Figure 7 G & H).

The ultrathin sections from the BPA plus Bone Marrow-Mesenchymal Stem Cells (BM-MSCs) group demonstrated a preservation of the alveolar tissue. The alveoli were patent (open) and maintained a lining composed of both types of pneumocytes. The type I pneumocytes exhibited an elongated, euchromatic nucleus, though a small degree of cytoplasmic vacuolation was noted. A macrophage characterized by lamellipodia and a kidney-shaped nucleus was observed within a capillary. The type II pneumocytes featured euchromatic nuclei but displayed a discernible perinuclear space, contained multiple lamellar bodies with only minimal vacuolation, and retained their typical microvillous border (Figures 7 I and J).

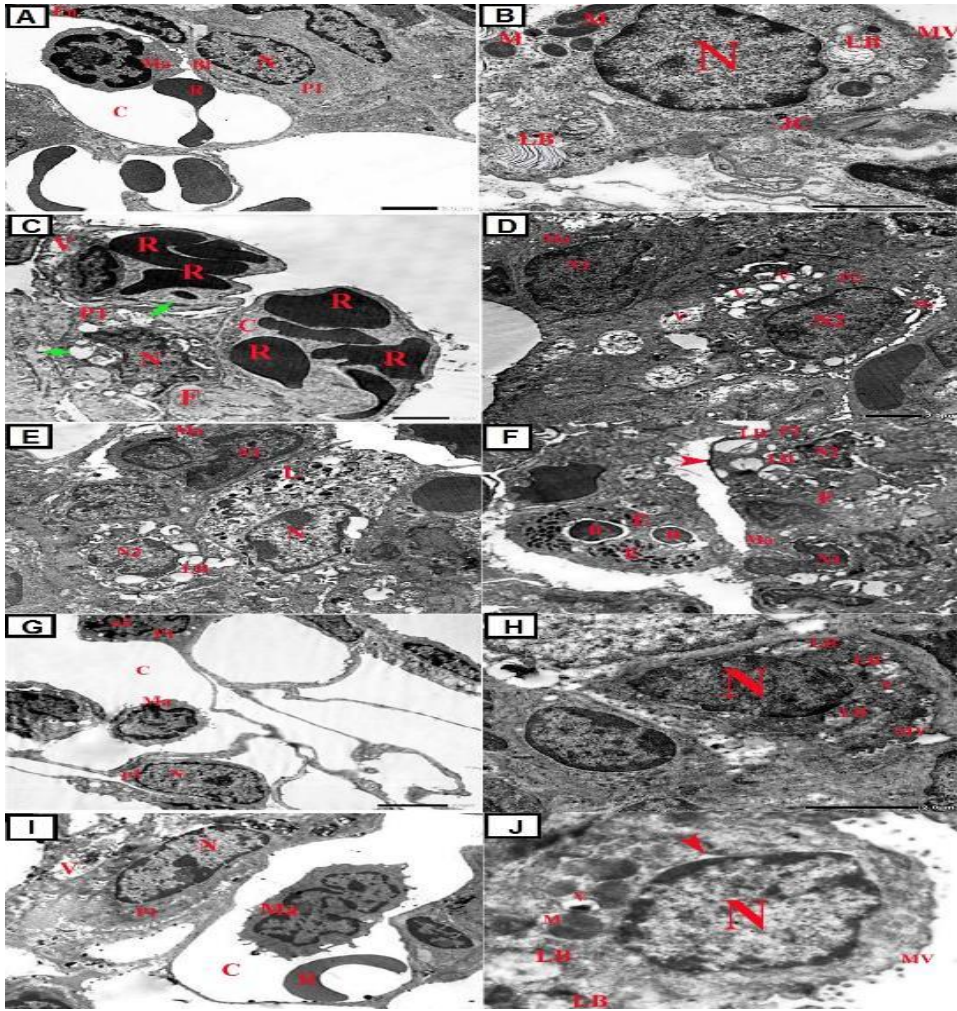


Fig.(7): Electron micrograph of the rat lung.

(A) Group I (control group) demonstrated patent alveoli, Intact blood air barrier consisting of endothelial cells (En) lining blood capillaries (C) within the interalveolar septum, capillary lumen contained blood Monocyte (Ma) and RBCs (R), Pneumocytes type I (PI) with flat euchromatic nucleus (N) and thin rim of cytoplasm, fused basal lamina (Bl) of endothelial and pneumocytes I.(x2000). (B) Group I (control group) showed pneumocytes type II (PII) with rounded euchromatic nucleus (N), cytoplasm contained lamellar bodies (LB), mitochondria (M), apical border showing microvilli (MV), while lateral border showed junctional complex (JC) (x4000). (C) Group III (BPA group) illustrated congested blood capillaries (C) with increased RBCs (R), lined by endothelial cell containing vacuoles (v), type 1 pneumocytes (p1) with irregular heterochromatic nucleus (n), multiple vacuoles within cytoplasm (green arrow) and increased collagen fibers (F) within interalveolar septum was noticed (x2000). (D) Group III (BPA group) demonstrateed pneumocyte type II (P2) with heterochromatic nucleus (N2), cytoplasm contained multiple vacuolated mitochondria and lamellar bodies (V), alveolar macrophage (Ma) with kidney shaped nucleus (N1), type II pneumocyte with irregular shrunken heterochromatic nucleus (N2) and cytoplasm contained empty lamellar bodies (LB) (x2000). (E) Group III

(BPA group) exhibited alveolar macrophage (Ma) with inactive kidney shaped heterochromatic nucleus (N1), another macrophage with active nucleus (N), multiple lysosomes (L), type II pneumocyte (P2) with irregular nucleus (N2) & empty lamellar bodies (LB) within cytoplasm (**x2000**). **(F)** Group III (BPA group) revealed Esionophil (E) wihin alveolar lumen with 2 nuclei (n) & multiple granules (g), alveolar macrophage (Ma) with kidney shaped heterochromatic nucleus (N1), type II pneumocyte (P2) with shrunken irregular heterochromatic nucleus (N2), empty lamellar bodies (LB) within cytoplasm and increased collagen fibers (F) was noticed (x2000). (G) Group IV (BPA plus melatonin group) showed thin interalveolar septum (I), pneumocytes type I (PI) with flat euchromatic nucleus (N), thin rim of cytoplasm, another pneumocyte type 1 (p1) with irregular heterochromatic nucleus (N2) and capillary (c) containing macrophage (Ma) (x2000). (H) Group IV (BPA plus melatonin group) showed pneumocytes type II (PII), euchromatic nucleus (N) with mild irregularity, cytoplasm contains lamellar bodies (LB), few vacuoles (V) and apical border that showed slightly blunted microvilli (MV) (x4000). (I) Group V (BPA plus BM-MSCs group) showed intact blood air barrier consisting of endothelial cells (En) lining blood capillaries (C) within the interalveolar septum, capillary lumen contained blood macrophage (Ma) and RBCs

(R), pneumocytes type I (PI) with flat euchromatic nucleus (N) and thin rim of cytoplasm but contains few vacuoles (V) (x2000). (J) Group V (BPA plus BM-MSCs group) showe pneumocytes type II (PII) with rounded euchromatic nucleus (N) but with slight perinuclear space (arrow head), cytoplasm contained lamellar bodies (LB), mitochondria (m), apical border showing slightly short microvilli (MV), but there was few vacuoles (V) (x4000).

DISCUSSION

Lung lipid peroxidation, oxidative stress, fibrosis and inflammation were the main findings in the current BPA group. The highly significant increase in MDA and highly significant decrease in GSH & SOD in the BPA group as compared to the control group. In addition BPA group illustrated histological alterations in the form of lung interstitium consolidation, significant inflammatory cellular infiltration, collapsed alveoli, extravasated RBCs, inflammatory cells such as eosinophils in the alveolar spaces, thickened interalveolar septum that contain congested dilated capillaries with inflammatory cells, acidophilic homogeneous material in lung interstitium and increased amount of collagen fibers in the interalveolar septa, around bronchi and around blood vessels. The light microscopic findings were further confirmed by marked alterations of the ultra-thin sections of the lung tissue that revealed marked alterations of alveolar architecture and the interalveolar septa appeared thickened having collagen fibers.

The mentioned findings are synchronous with the study of Morsi et al. [18] that demonstrated a remarkable increase in MDA, decrease in SOD activity in BPAexposed group with apparent histopathological changes and extensive fibrosis marked by a peribronchial, perivascular and interstitial accumulation of coarse collagen fibers. Moreover, Abedelhaffez et al. [19] discovered similar results to histological findings in the current study in the form of congested thickened pulmonary arteries with extravasated red blood cells, inflammatory cell infiltration and collapsed alveoli in tissues of lung treated with BPA. Eweda et al. [20]. also assumed that BPA administration resulted in increased MDA content within the tissues resulting in oxidative damage with decreased antioxidants such as SOD, glutathione peroxidase, and glutathione-S-transferase. These antioxidants share by a critical role in destruction of the formed ROS due to oxidative stress. Therefore, ROS overproduction and antioxidants depletion occurs resulting in disturbance of endogenous antioxidant defenses leading to tissue damage. Similarly, Rehman et al. [21] reported rat lung inflammation and oxidative stress that was induced by BPA. Furthermore. Attia et al. [22] attributed the existing changes to increased oxidative stress, hazardous free radical generation and ROS formation. These oxygen radicals' byproducts are cytotoxic agents as they attack biomolecules like membrane lipids, DNA, RNA, and

proteins leading to progressive oxidative destruction, resulting in cell death and apoptosis.

Thickened interalveolar septum in the current study could be related to an increase in the infiltration of numerous blood components such as macrophages and neutrophils, as documented by **Rehman** *et al.* ^[21] that BPA activates macrophages to release inflammatory cytokines that enhance neutrophil accumulation and migration outside blood vessel. This could explain the presence of macrophages noted in the current study.

Congested blood vessels might be attributed to rise in the proportion of oxygen supply to oxygen demand, resulting in an elevation in the adenosine generation. As a result, blood vessels dilate and blood flow increases, returning oxygen levels to normal [23].

Inflammatory cells infiltration detected in the current study might be mediated by proinflammatory cytokines, especially tumor necrosis factor α (TNF- α), that results in changes on the effects of other cytokines, such as interleukin 1β (IL-1β). ROS and free radicals produced due to oxidative stress induced by BPA result in proinflammatory cytokines TNF-α and IL-1β upregulation [24]. Increased ROS and proinflammatory cytokines activate nuclear factor kappa B (NF-kB) through kinase pathways. Nuclear factor kappa B (NF-kB) regulates chronic inflammation by influencing the transcription of several inflammatory genes, including cytokines and chemokines, which are responsible for the inflammatory changes seen in lung exposed to BPA [25]. Additionally, acidophilic homogeneous material in lung interstitium of BPA group might be attributed to the edema occurring as a result of inflammation [26]. These findings are supported by the strong positive cytoplasmic expression to TNF-α and COX-2 inflammatory markers in BPA group in the ongoing study.

The results from the present investigation, specifically the strong positive cytoplasmic expression of the inflammatory markers TNF-α and COX-2 observed within the group exposed solely to Bisphenol A (BPA) furnish substantial evidence that supports the preceding findings. Concurrently, other scholarly work by **Mohammed** *et al.* [27] established a mechanistic link, proposing that the noticeable increase in the quantity of collagen fibers was a direct consequence of augmented fibroblast activity coupled with cellular hyperplasia, which was itself a pathological response elicited by the exposure to BPA. The therapeutic agent under consideration, melatonin, exhibited a pronounced lipophilic characteristic, a physicochemical property that grants it the facility to readily permeate various biological barriers, including cellular and intracellular membranes. This ease of cellular access is vital for its functions. Melatonin is well-established in the literature for possessing potent antioxidant and anti-apoptotic attributes. Its protective mechanism against the detrimental effects induced by BPA

exposure may involve a multifaceted approach, notably by enhancing the biological system's inherent capacity for scavenging free radicals ^[28]. Additionally, prior research has demonstrated that melatonin is effective in ameliorating mitochondrial oxidative damage that is instigated by free radicals in female murine models ^[29]. This collective evidence underscores the potential of melatonin to neutralize multiple facets of BPA-induced pathology, ranging from inflammation and connective tissue overgrowth to direct cellular and organelle damage.

In the BPA plus melatonin group, the lung tissue demonstrated a significant recovery, re-establishing almost all of its normal histological features at both the light and electron microscopic levels. However, some residual pathological findings were still evident, specifically a slight thickening in the interalveolar septa, the persistence of a few congested blood capillaries within these septa, and a moderate quantity of collagen fibers distributed between the alveoli and surrounding the blood vessels.

The expression of the inflammatory biomarkers TNF-α and COX-2 was substantially less evident in the group treated with BPA plus melatonin when compared directly to the cohort receiving BPA alone. Moreover, this combined treatment group exhibited a significant decrease in the lipid peroxidation marker MDA and a corresponding significant elevation in the antioxidant capacity markers GSH and SOD activity relative to the singular BPA group. These observations collectively provide evidence indicating a potent antioxidative and anti-inflammatory action mediated by melatonin, specifically countering the pathological effects of BPA exposure. These compelling observations are consistent with existing evidence from the study conducted by Xiong et al. [30], which established that melatonin is capable of reducing lung tissue damage, apoptosis, and adverse inflammatory responses that are commonly induced by passive smoking. Furthermore, an investigation by another research group highlighted that the administration of melatonin to rats exposed to cigarette smoke led to significantly reduced systemic levels of the total antioxidant capacity. Crucially, this treatment also resulted in lower concentrations of key inflammatory markers such as TNF-α, Interleukin-6 (IL-6), and Interleukin-1 beta (IL-1\beta), with the mechanistic data suggesting that this protective effect is mediated by the inhibition of phosphodiesterase 4 in mice [31]. This comprehensive body of work reinforces the therapeutic role of melatonin in countering environmentally induced pathology and oxidative disturbances. Aminjan et al. [32] explained that melatonin has both direct and indirect pathways as it can directly neutralize free radicals and related toxicants, so it protects antioxidative enzymes from oxidative damage. Every molecule of melatonin neutralizes two hydroxyl-free radicals. Melatonin can also reduce the production of free radicals and electron leakage, while boosting the effectiveness of mitochondrial electron transport.

Moreover, **BPA** plus BM-MSCs demonstrated histological features similar to the control group, however few congested blood capillaries were still present within thin interalveolar septa. a very minimal amount of collagen fibers in interalveolar septa and ultrathin sections revealed preservation of the alveolar tissue. TNF-α and COX-2 expressions were minimal. This observed improvement is in agreement with previous studies that reported regression of the inflammatory and fibrotic responses after MSCs administration in the bleomycin-induced pulmonary fibrosis in rodents [33] and that hold a promising therapeutic effect of BM-MSCs for treatment of lung fibrosis due to their distinctive regenerative, anti-apoptotic and anti-inflammatory effects [12]. Various mechanisms explained the repair of damaged lung tissue by BM-MSCs. Savukinas et al. [34] stated that fibrosis resolution was accelerated through epithelial restitution and added that stem cells renovate the organization of the cytoskeleton of the alveolar epithelium. Moreover, MSCs facilitate the regeneration of endothelial cells and restoration of vascular integrity in lung tissue. Additionally, MSCs suppress apoptosis, release growth cytokines and stimulate cellular regeneration and differentiation in damaged lung areas [34]. Furthermore, it has been documented that the paracrine secretion of MSCs serves a vital part in repair process of lung fibrosis by reducing inflammation and fibrosis. Furthermore, MSCs secrete immunosuppressive molecules that stimulate conversion of pro-inflammatory macrophages to antiinflammatory ones. In addition, MSCs secrete matrix metalloproteinase, an enzyme that directly breaks down the extracellular matrix, thereby facilitating the clearance of fibrosis [35].

CONCLUSION

The current study reported that BPA induced lung fibrosis and inflammation in rats. BM-MSCs and melatonin significantly improved such fibrosis and inflammation as proved by biochemical, histological and morphometrical studies. The findings illustrated a more obvious improvement in response to BM-MSCs than melatonin pointing to its potential future application as a therapeutic modality to attenuate lung fibrosis and inflammation.

Conflicts of Interest: No conflicts of interest that influenced this paper.

Funding: None.

REFERENCES

- 1. Manzoor M, Tariq T, Fatima B *et al.* (2022): An insight into bisphenol A, food exposure and its adverse effects on health: a review. Front Nutr., 9: 1047827.
- Segovia-Mendoza M, Nava-Castro K, Palacios-Arreola M et al. (2020): How microplastic components influence the immune system and impact on children health: Focus on cancer. Birth Defects Res., 112 (17): 1341-1361.

- **3. Shi Y, Chen W, Du Y** *et al.* (2023): Damage Effects of Bisphenol A against Sepsis Induced Acute Lung Injury. Gene, 878: 147575.
- **4. Sirasanagandla S, Al-Huseini I, Sakr H** *et al.* **(2022):** Natural products in mitigation of bisphenol A toxicity: future therapeutic use. Molecules, 27 (17): 5384.
- Aysin F (2024): Bisphenol A promotes cell death in healthy respiratory system cells through inhibition of cell proliferation and induction of G2/M cell cycle arrest. Environ Toxicol., 39 (5): 3264-3273.
- **6. Moustafa E, Ibrahim S, Salem F (2020):** Methylsulfonylmethane inhibits lung fibrosis progression, inflammatory response,and epithelial-mesenchymal transition via the transforming growth factor-B1/SMAD2/3 pathwayin rats exposed to both γ-radiation and Bisphenol-A. Toxin Rev., 40 (4): 1431-1440.
- Kobayashi K, Liu Y, Ichikawa H et al. (2020): Effects of Bisphenol A on Oxidative Stress in the Rat Brain. Antioxidants (Basel), 9 (3): 240.
- **8. Knight A, Kacker S (2023):** Platelet-Rich Plasma Treatment for Chronic Respiratory Disease. Cureus, 15 (1): e33265.
- **9. Nabavi** S, Nabavi S, Sureda A *et al.* (2019): Antiinflammatory effects of Melatonin: A mechanistic review. Crit Rev Food Sci Nutr., 59 (1): S4-S16.
- **10.** Wang W, Gao J (2021): Effects of melatonin on protecting against lung injury (Review). Exp Ther Med., 21 (3): 228.
- 11. Rostom D, Attia N, Khalifa H et al. (2020): The therapeutic potential of extracellular vesicles versus mesenchymal stem cells in liver damage. Tissue Eng Regen Med., 17 (4): 537-552.
- **12. Boughdady W, Hegab Z, Mohamed D (2024):** Therapeutic Effect of Bone Marrow Derived Mesenchymal Stem Cells Versus Platelet Rich Plasma on Amiodarone Induced Lung Fibrosis in Adult Male Albino Rat: Histological Study. EJH., 47 (4): 1325-1342.
- **13. Alboghobeish S, Mahdavinia M, Zeidooni L** *et al.* **(2019):** Efficiency of naringin against reproductive toxicity and testicular damages induced by bisphenol A in rats. Iran J Basic Med Sci., 22 (3): 315-523.
- **14. Khorsand M, Akmali M, Akhzari M (2019):** Efficacy of melatonin in restoring the antioxidant status in the lens of diabetic rats induced by streptozotocin. J Diabetes Metab Disord., 18 (2): 543-549.
- **15. Faheem N, El Askary A, Gharib A (2021):** Lycopene attenuates bisphenol A-induced lung injury in adult albino rats: a histological and biochemical study. Environ Sci Pollut Res Int., 28 (35): 49139-49152.
- **16. Suvarna S, Layton C, Bancroft J (2019):** Connective tissue stains: Bancroft's Theory and Practice of Histological Techniques, 8th ed. Elsevier, Churchill Livingstone, Edinburgh, London, Oxford, New York, Philadelphia, St Louis, Sydney and Toronto, Pp: 199-212.
- **17. Bozzola J** (2007): Conventional specimen preparation techniques for transmission electron microscopy of cultured cells. Methods Mol Biol., 369: 1-18.
- **18.** Morsi A, Mersal E, Abdelmoneim A *et al.* (2023): ACE2/ACE imbalance mediates bisphenol A-induced lung injury in Wistar rats: Results from captopril versus losartan histo-biochemical study. Heliyon, 9 (11): e22056.
- 19. Abedelhaffez A, Abd El-Aziz E, Abdel Aziz M et al. (2017): Lung injury induced by bisphenol A: a food

- contaminant, is ameliorated by selenium supplementation. Pathophysiology, 24 (2): 81-89.
- **20.** Eweda S, Newairy A, Abdou H *et al.* (2020): Bisphenol A induced oxidative damage in the hepatic and cardiac tissues of rats: The modulatory role of sesame lignans. Exp Ther Med., 19 (1): 33-44.
- **21. Rehman A, Akhtar T, Hameed N** *et al.* **(2021):** In vivo assessment of bisphenol A induced histopathological alterations and inflammatory gene expression in lungs of male Wistar rats. Hum Exp Toxicol., 40 (3): 538-549.
- 22. Attia Z, Mostafa H, Allam Z (2021): Ameliorative effect of curcumin on the toxicity induced by bisphenol A on brain of male albino rats. Nat Sci., 19 (1): 19-24.
- 23. Tolba A, Mandour D (2018): Histological effects of bisphenol-A on the reproductive organs of the adult male albino rat. Eur J Anat., 22 (2): 89-102.
- **24.** Caldeira D, Weiss D, Rocco P *et al.* (2021): Mitochondria in Focus: From Function to Therapeutic Strategies in Chronic Lung Diseases. Front Immunol., 12: 782074.
- **25.** Muhammed M, Mostafa R, Said M et al. (2021): Protective Effect of Thymoquinone on Bisphenol A-Induced Hepatotoxicity in Male Rats, Targeting the Role of Associated Pro-Inflammatory Cytokines and NF-kB. Benha Med J., 38: 61-72.
- **26.** Omorodion N, Atoigwe-Ogeyemhe B, Achukwu P *et al.* (2019): Histopathological changes associated with exposure of some viscerals and testicular tissues to bisphenol A and di(2-ethylhexyl) phthalate. Trop J Pharm Res., 18 (6): 1213-1218.
- 27. Mohammed H, Al-sayed A, Abulfadle K et al. (2019): Potential Protective Role of Vitamin E in Lung of Adult Male Albino Rat Exposed to Bisphenol A. Med J Cairo Univ., 87 (8): 4901-4915.
- **28.** Tamura H, Jozaki M, Tanabe M *et al.* (2020): Importance of melatonin in assisted reproductive technology and ovarian aging. Int J Mol Sci., 21 (3): 1135.
- **29. Olcese J (2020):** Melatonin and female reproduction: an expanding universe. Front Endocrinol., 11: 85.
- **30. Xiong J, Xie L, Huang Y** *et al.* **(2024):** Therapeutic effects of melatonin on the lungs of rats exposed to passive smoking. Respir Res., 25: 411.
- **31.** Lim J, Kim W, Lee S *et al.* (2021): The involvement of PDE4 in the protective effects of melatonin on cigarette-smoke-induced chronic obstructive pulmonary disease. Molecules, 26 (21): 6588.
- **32. Aminjan H, Abtahi S, Hazrati E** *et al.* **(2019):** Targeting of oxidative stress and inflammation through ROS/NFkappaB pathway in phosphine-induced hepatotoxicity mitigation. Life Sci., 232: 116607.
- **33.** Chen X, Wu Y, Wang Y *et al.* (2020): Human menstrual bloodderived stem cells mitigate bleomycin-induced pulmonary fibrosis through anti-apoptosis and anti-inflammatory effects. Stem Cell Res Ther., 11 (1): 477.
- **34.** Savukinas U, Enes S, Sjoland A *et al.* (2016): Concise review: the bystander effect: mesenchymal stem cell-mediated lung repair. Stem Cells, 34 (6): 1437-1444.
- **35. Abdel Halim A, Ahmed H, Aglan H** *et al.* **(2021):** Role of bone marrow-derived mesenchymal stem cells in alleviating pulmonary epithelium damage and extracellular matrix remodeling in a rat model of lung fibrosis induced by amiodarone. Biotech Histochem., 96 (6): 418-430.